Arterial wall tethering as a distant boundary condition

S. Hodis[1] and M. Zamir[1,2]
[1]*Department of Applied Mathematics, University of Western Ontario, London, Canada N6A 5B7*
[2]*Department of Medical Biophysics, University of Western Ontario, London, Canada N6A 5B7*
(Received 22 May 2009; revised manuscript received 25 September 2009; published 18 November 2009)

A standing difficulty in the problem of blood vessel tethering has been that only one of the two required boundary conditions can be fully specified, namely, that at the inner (endothelial) wall surface. The other, at the outer layer of the vessel wall, is not known except in the limiting case where the wall is fully tethered such that its outer layer is prevented from any displacement. In all other cases, where the wall is either free or partially tethered, a direct boundary condition is not available. We present a method of determining this missing boundary condition by considering the limiting case of a semi-infinite wall. The result makes it possible to define the degree of tethering imposed by surrounding tissue more accurately in terms of the displacement of the outer layer of the vessel wall, rather than in terms of equivalent added mass which has been done in the past. This new approach makes it possible for the first time to describe the effect of partial tethering in its full range, from zero to full tethering. The results indicate that high tethering leads to high stresses and low displacements within the vessel wall, while low tethering leads to low stresses and high displacements. Since both extremes would be damaging to wall tissue, particularly elastin, this suggest that moderate tethering would be optimum in the physiological setting.

DOI: 10.1103/PhysRevE.80.051913 PACS number(s): 87.19.ug

I. INTRODUCTION

Arterial tethering, the effect of surrounding tissue on the free movement of the arterial wall, has been investigated for some time, but no satisfactory method of modeling this effect has been established [1]. The "added mass" concept introduced by Womersley [2] and Morgan [3] works well for a thin vessel wall in which stress and displacement are assumed to be independent of position within the wall thickness. The aim of this paper is to relax this assumption in order to actually explore the distributions of stress and displacement within the thickness of the vessel wall.

As a result of pulsatile flow, blood vessels are subject to two principal forces, namely, pressure in the radial direction and shear force in the axial direction. Focus in the past has been largely on the effects of radial forces [1,4,5]. In this paper we focus on forces in the axial direction because it has been shown recently that displacements in that direction are as significant as those in the radial direction [5]. Also, displacements in the axial direction are driven by the shear force exerted by pulsatile flow on endothelial tissue, which is then transmitted to other layers of the vessel wall, thus creating a field of shear stresses within the wall which as yet have not been fully explored. Here the extent to which the vessel is tethered is particularly critical because it determines the magnitude of these stresses and their distribution within the wall thickness.

The extent of tethering can be quite different in different parts of the vascular system. In the case of cerebral arteries which are surrounded by cerebrospinal fluid, there is very little tethering and the vessels are fairly free to move [6]. In the case of coronary arteries, by contrast, the vessels are highly tethered to surrounding tissue, many being imbedded within the myocardium. The issue of partial tethering is therefore important but there has not been an effective way of dealing with it in the past in terms of either the concept of added mass [2,3] or that in which tethering is viewed as stress response of the surrounding medium on the outer layer of the vessel wall [1,7–9]. Indeed, the definition of partial tethering in these terms is rather difficult. In this paper we propose a definition of partial tethering in terms of displacement of the outer layer of the vessel wall and use that definition to determine the longitudinal stresses and displacements within the thickness of the vessel wall.

II. LONGITUDINAL TETHERING DEFINED

While tethering is clearly defined in the two extreme and rather idealized cases where the outer layer of the vessel wall is either entirely free from or completely restrained by surrounding tissue, a definition is lacking in the more relevant cases of partial tethering where the outer layer of the vessel wall is not completely restrained nor entirely free. The concepts of added mass or of changed parameter values in the governing equations which have been used in the past [8,9] do not provide a practical measure of partial tethering because neither the added mass nor the parameter values can be adequately interpreted or estimated in the physiological situation.

We propose a definition of tethering based on the longitudinal displacement of the outer layer of the vessel wall, which recent advances in imaging technology have made it possible to not only visualize but actually measure [10].

It is important to recognize that when the vessel wall is entirely free from tethering by surrounding tissue, the outer layer of the wall undergoes some nonzero displacement as a result of the oscillatory shear force at the inner wall layer. We denote the non-time-dependent coefficient of that displacement by $\xi_{1,0}$, the first subscript referring to the outer layer of the wall, and the second denoting zero tethering, and use this as a baseline for the corresponding coefficient of displacement of the outer layer of the wall when the wall is

not entirely free from surrounding tissue, the latter being denoted by $\xi_{1,\delta}$, where δ refers to the presence of nonzero tethering.

The ratio $|\xi_{1,\delta}|/|\xi_{1,0}|$ is now used to define a degree of tethering δ, ranging in value from 0 when the wall is free to 1.0 when the wall is fully tethered, namely,

$$\delta = 1 - \frac{|\xi_{1,\delta}|}{|\xi_{1,0}|}. \tag{1}$$

The absolute value signs indicate that in general both $\xi_{1,0}$ and $\xi_{1,\delta}$ may be complex because of the wall material. At this stage both $\xi_{1,\delta}$ and $\xi_{1,0}$ are unknown. In what follows we present an analytical solution of the governing equation first to find $\xi_{1,0}$ and then to determine $\xi_{1,\delta}$ for any prescribed degree of tethering.

III. ANALYTICAL PROBLEM: UNKNOWN BOUNDARY CONDITION

Analytically, the problem of tethering can be posed as a solution of a second-order differential equation in the axial displacement $\xi(r,t)$ of material elements of the vessel wall [14],

$$\rho \frac{\partial^2 \xi}{\partial t^2} = E^* \left[\frac{\partial^2 \xi}{\partial r^2} + \frac{1}{r} \frac{\partial \xi}{\partial r} \right], \tag{2}$$

where r is the radial coordinate, t is time, ρ is density of the wall material, and E^* is complex viscoelasticity modulus which depends on the mechanical properties of the wall [15]. This equation is a simplified form of the full equations governing viscoelastic motion in a three-dimensional medium, using simplifying assumptions generally used for the vessel wall and in particular the assumption that the length of the propagating wave is much larger than the vessel length [14,1]. Solution of the full equations in all three dimensions becomes intractable because of the number of unknown coefficients involved, which practically eliminate the possibility of an analytical solution [11–13]. The focus in the present paper is on the tethering problem outlined in the Introduction, which arises principally in the longitudinal direction because of the forces of pulsatile flow in that direction. This problem is hence appropriately captured in Eq. (2). This equation also offers the advantage of an analytical solution which facilitates the discussion and ultimate resolution of the missing boundary-condition problem.

The difficulty with the solution of Eq. (2) has been that only one of the two required boundary conditions can be fully specified, namely, that at the inner (endothelial) wall surface where the no-slip boundary condition requires that the blood velocity and wall velocity be the same, which thus provides a boundary condition at $r=a$ in terms of $\xi(a,t)$, where a is the vessel radius. The other boundary condition, at $r=a+h$, where h is the wall thickness, is not known except in the limiting case where the wall is fully tethered to the extent that its outer layer is prevented from any displacement, which thus provides the boundary condition $\xi(a+h,t)=0$. In all other cases, where the wall is either free or partially tethered, a direct boundary condition is not available.

Consider first an inner boundary condition of the form

$$\xi(a,t) = \xi_0 e^{i\omega t}, \tag{3}$$

where ξ_0 and ω are the amplitude and frequency of a single harmonic oscillation, which may be considered as one component of an oscillatory flow waveform [16]. If the wall material is assumed to be homogeneous, displacements and stresses throughout the wall thickness will have the same oscillatory form as, though in general not in phase with, oscillations at the inner boundary. In particular, longitudinal displacement of the outer layer of the wall will have the form

$$\xi(a+h,t)|_\delta = \xi_{1,\delta} e^{i\omega t}, \tag{4}$$

where $\xi_{1,\delta}$ is the unknown, generally complex, non-time-dependent coefficient of displacement of the outer layer of the wall introduced in the previous section. The general solution of Eq. (2) is of the form

$$\bar{\xi}(r,t) = [AI_0(\zeta) + BK_0(\zeta)]e^{i\omega t}, \tag{5}$$

where I_0 and K_0 are modified Bessel functions of order zero of first and second kind, respectively, and A and B are constants of integration determined from the two boundary conditions

$$A = A_1 = \frac{K_0(\zeta_1) - K_0(\zeta_0)|\bar{\xi}_{1,\delta}|}{K_0(\zeta_1)I_0(\zeta_0) - I_0(\zeta_1)K_0(\zeta_0)},$$

$$B = B_1 = -\frac{I_0(\zeta_1) - I_0(\zeta_0)|\bar{\xi}_{1,\delta}|}{K_0(\zeta_1)I_0(\zeta_0) - I_0(\zeta_1)K_0(\zeta_0)}, \tag{6}$$

and

$$\bar{\xi} = \xi/\xi_0, |\bar{\xi}_{1,\delta}| = |\xi_{1,\delta}|/\xi_0,$$

$$\zeta = \Lambda(\bar{r} + a/h), \zeta_0 = \Lambda a/h, \zeta_1 = \Lambda(a+h)/h,$$

$$\bar{r} = (r-a)/h,$$

$$\Lambda = \omega h \sqrt{\rho/E^*}. \tag{7}$$

The solution in Eq. (5) with the constants A_1 and B_1 is incomplete because of the unknown coefficient $\xi_{1,\delta}$ which appears in the constants of integration. Note that because the viscoelasticity modulus E^* is complex and hence so is Λ and ζ, the displacements in Eq. (5), will in general be out of phase with that of the inner boundary in Eq. (3).

IV. CURRENT METHOD OF DEALING WITH TETHERING

Modeling the stress exerted by surrounding tissue was introduced by Patel in 1966 [7] in which the stress was

represented by a spring, a dashpot, and a lumped mass in general, but in the case of a free vessel only the inertial component was taken [7–9]. The model was widely used by others, to study the radial stress [1], using the assumption that the wall thickness was small enough that the stress was uniform [8], or using a numerical scheme to solve the problem [9].

In the case of a free vessel, the shear stress at the outer boundary was taken as [7]

$$\tau(a+h,t) = \rho h \frac{\partial^2 \xi}{\partial t^2}, \tag{8}$$

which is an approximation of the full equation of motion of material elements within the vessel wall, namely, [14]

$$\rho \frac{\partial^2 \xi(r,t)}{\partial t^2} = \frac{\partial \tau(r,t)}{\partial r} + \frac{\tau(r,t)}{r}. \tag{9}$$

The term $\partial\tau(r,t)/\partial r$ represents the shear stress variation within the wall thickness and it was omitted in Eq. (8) on the grounds that the wall is sufficiently thin. In the present study we retain this term in order to actually explore the shear stress variation within the vessel wall with different degrees of tethering. The solution we seek is based on the full equation of motion [Eq. (9)], which in terms of displacement is that given in Eq. (2).

V. LIMIT OF TETHERING AT INFINITY

We present a method of dealing with the unknown outer boundary condition for the free vessel wall by considering the limiting case of a semi-infinite wall fully tethered at infinity and solve Eq. (2) together with the inner boundary condition in Eq. (3). In fact, since the general solution of Eq. (2) already given in Eq. (5) is not restricted to a finite wall, it applies in this case too. In order to satisfy the outer boundary condition at infinity, however, the solution must meet the requirement that

$$\lim_{r\to\infty} |\bar{\xi}(r,t)| = \lim_{r\to\infty} |AI_0(\zeta) + BK_0(\zeta)||e^{i\omega t}| = 0. \tag{10}$$

Now since

$$\lim_{r\to\infty} |I_0(\zeta)| = \infty, \tag{11}$$

it follows that $A=0$ and using the inner boundary condition in Eq. (3), the other constant is given by

$$B = \frac{1}{K_0(\zeta_0)}. \tag{12}$$

Thus, the displacement at any radial position r in the semi-infinite wall is given by

$$\bar{\xi}(r,t) = \frac{1}{K_0(\zeta_0)} K_0(\zeta) e^{i\omega t}. \tag{13}$$

In fact, the same results can be reached in this case without imposing the fully tethered boundary condition at infinity, using instead what has been termed the "radiation condition" [17]. Briefly, the governing equation [Eq. (2)] is a hyperbolic (wave) equation in which the two terms in the general solution [Eq. (5)] represent waves moving in the positive (B-term) and negative (A-term) r directions. The latter is zero in this case because of the absence of any source of wave reflections at a finite distance from the inner boundary ($r=a$). Thus the term representing such waves in the general solution is zero, leading to the results in Eqs. (12) and (13).

VI. UNTETHERED WALL: PROPOSED SOLUTION

From the solution for a semi-infinite wall in the previous section, the displacement of any layer of the wall at a distance $r-a$ from the inner boundary can be calculated. Since in that solution, tethering is applied at an infinite distance from the inner boundary, however, its effect at finite distances from the inner boundary is zero. Thus, in the semi-infinite wall, displacements obtained at finite distances from the inner boundary are not due to the tethering at infinity but to the inner boundary condition only. In other words, they are the displacements that would be produced in an *untethered* wall of finite thickness, because in both the finite free wall and the semi-infinite tethered wall the displacements at finite distances from the inner boundary are produced by the inner boundary condition only. In particular, the displacement at the outer layer $r=a+h$ of an untethered wall, using Eqs. (13), (4), and (7) can be obtained from

$$\bar{\xi}(a+h,t)|_{\delta=0} = \bar{\xi}_{1,0} e^{i\omega t} = \frac{K_0(\zeta_1)}{K_0(\zeta_0)} e^{i\omega t}, \tag{14}$$

hence

$$\bar{\xi}_{1,0} = \frac{\xi_{1,0}}{\xi_0} = \frac{K_0(\zeta_1)}{K_0(\zeta_0)}, \tag{15}$$

where $\bar{\xi}_{1,0}$ is the non-time-dependent coefficient of displacement at the outer layer of an untethered wall ($\delta=0$) of thickness h, which thus provides the missing boundary condition required for the finite untethered wall.

VII. PARTIAL TETHERING

With the definition of δ in Eq. (1) and the value of $\bar{\xi}_{1,0}$ in Eq. (15), the material constants A_1, B_1 from Eq. (6) are now fully determined for any degree of tethering, namely,

$$A_1 = \frac{K_0(\zeta_1) - K_0(\zeta_0)(1-\delta)|\bar{\xi}_{1,0}|}{K_0(\zeta_1)I_0(\zeta_0) - I_0(\zeta_1)K_0(\zeta_0)},$$

$$B_1 = -\frac{I_0(\zeta_1) - I_0(\zeta_0)(1-\delta)|\bar{\xi}_{1,0}|}{K_0(\zeta_1)I_0(\zeta_0) - I_0(\zeta_1)K_0(\zeta_0)}. \tag{16}$$

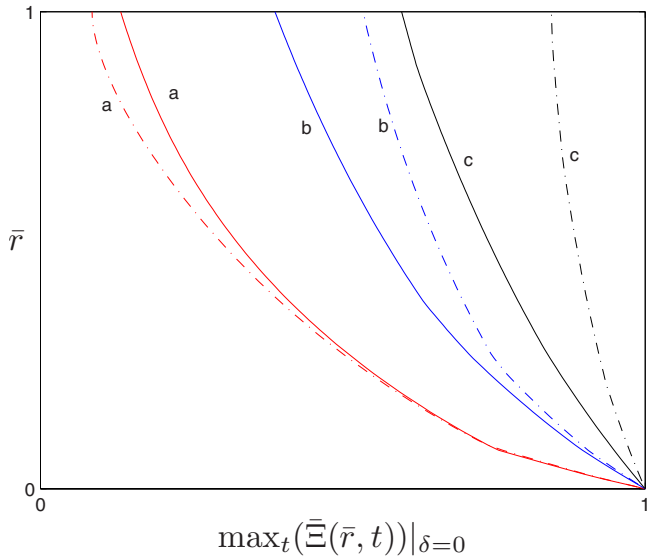

FIG. 1. (Color online) Displacement amplitude (within one oscillatory cycle) at different depths within the thickness of an untethered wall as determined from the limiting solution in Eq. (22) with tethering at infinity (solid) compared with the approximate results in Eq. (32) (dashed) for the viscous (a), viscoelastic (b), and rigid (c) materials defined in Table I.

To find the stress distribution $\tau(r,t)$ at different layers of the vessel wall, we use the constitutive relationship [14]

$$\tau = E^* \frac{\partial \xi}{\partial r} \tag{17}$$

and using Eq. (5), the stress in normalized form is given by

$$\bar{\tau}(r,t) = \lambda\Lambda[A_1 I_1(\zeta) - B_1 K_1(\zeta)]e^{i\omega t}, \tag{18}$$

where I_1, K_1 are modified Bessel functions of order one of first and second kind, respectively, and

$$\bar{\tau} = \frac{\tau h}{\xi_0 E_1}, \tag{19}$$

$$\lambda = E^*/E_1. \tag{20}$$

Unlike the displacements, which are normalized in terms of the displacement at the inner boundary [Eq. (7)], the shear stress is here normalized in terms of a constant elastic modulus E_1 because the shear stress at the inner boundary, $\tau(a,t)$, is different for different materials. In the results to follow we take E_1=0.411 MPa [15].

VIII. GENERALIZATION TO PHYSIOLOGICAL WAVEFORM

To generalize these results to a physiological form of pulsatile blood flow where the displacement at the inner wall is a composite waveform derived from a cardiac pressure wave, we consider an inner layer boundary condition as the sum of ten harmonics

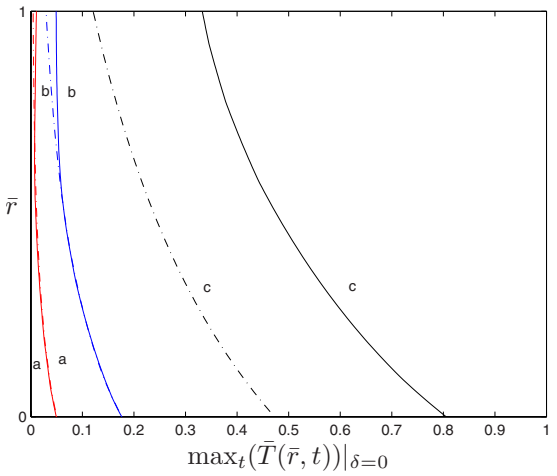

FIG. 2. (Color online) Shear stress amplitude (within one oscillatory cycle) at different depths within the thickness of an untethered wall as determined from the limiting solution in Eq. (23) with tethering at infinity (solid) compared with the approximate results in Eq. (33) (dashed), for the viscous (a), viscoelastic (b), and rigid (c) materials defined in Table I.

$$\Xi(a,t) = \sum_{n=1}^{n=10} M_n \cos(n\omega t) + N_n \sin(n\omega t), \tag{21}$$

where M_n, N_n are Fourier coefficients of a composite waveform given in [16].

The displacement and stress distributions based on this boundary condition and *for any degree of tethering*, using Eqs. (5) and (18), are then given by

$$\bar{\Xi}(r,t) = \frac{1}{\Xi_0}\sum_{n=1}^{10} M_n \Re\{[A_{1n} I_0(\zeta_n) + B_{1n} K_0(\zeta_n)]e^{in\omega t}\} + \frac{1}{\Xi_0}\sum_{n=1}^{10} N_n \Im\{[A_{1n} I_0(\zeta_n) + B_{1n} K_0(\zeta_n)]e^{in\omega t}\} \tag{22}$$

and

$$\bar{T}(r,t) = \frac{1}{\Xi_0}\sum_{n=1}^{10} M_n \Re\{\Lambda_n\lambda_n[A_{1n} I_1(\zeta_n) - B_{1n} K_1(\zeta_n)]e^{in\omega t}\} + \frac{1}{\Xi_0}\sum_{n=1}^{10} N_n \Im\{\Lambda_n\lambda_n[A_{1n} I_1(\zeta_n) - B_{1n} K_1(\zeta_n)]e^{in\omega t}\}, \tag{23}$$

where A_{1n} and B_{1n} (n=1 to 10) are given by

$$A_{1n} = \frac{K_0(\zeta_{1n}) - K_0(\zeta_{0n})(1-\delta)\bar{\Xi}_{1,0}}{K_0(\zeta_{1n})I_0(\zeta_{0n}) - I_0(\zeta_{1n})K_0(\zeta_{0n})},$$

$$B_{1n} = -\frac{I_0(\zeta_{1n}) - I_0(\zeta_{0n})(1-\delta)\bar{\Xi}_{1,0}}{K_0(\zeta_{1n})I_0(\zeta_{0n}) - I_0(\zeta_{1n})K_0(\zeta_{0n})}, \tag{24}$$

$$\zeta_n = \Lambda_n r/h, \quad \zeta_{0n} = \Lambda_n a/h, \zeta_{1n} = \Lambda_n(a+h)/h,$$

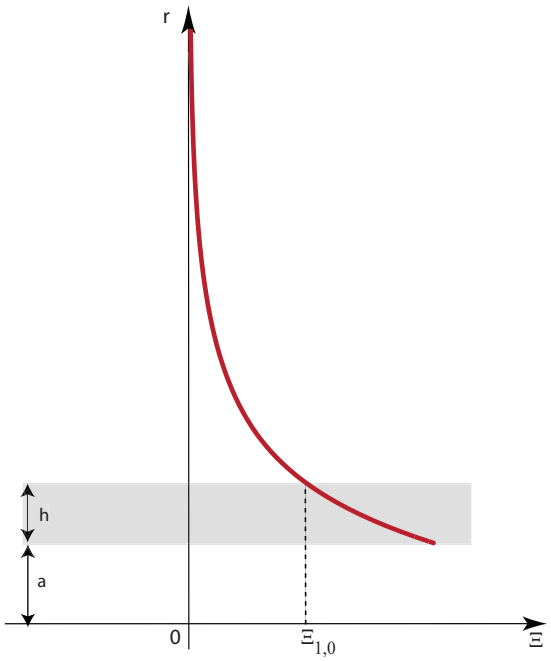

FIG. 3. (Color online) The way in which the displacement of the outer layer of an untethered wall of thickness h is obtained from the limiting case of a semi-infinite wall fully tethered at infinity (bold), thus providing the missing outer boundary condition for the former.

$$\Lambda_n = n\omega h\sqrt{\rho/E_n^*},$$

$$\lambda_n = E_n^*/E_1, \tag{25}$$

and

$$\Xi_0 = \max_t[\Xi(a,t)], \tag{26}$$

$$\bar{\Xi}_{1,0} = \max_t \bar{\Xi}(a+h,t)|_{\delta=0} = \max_t\left(\frac{1}{\Xi_0}\sum_{n=1}^{10}\left\{M_n\Re\left[\frac{K_0(\zeta_{1n})}{K_0(\zeta_{0n})}e^{in\omega t}\right] + N_n\Im\left[\frac{K_0(\zeta_{1n})}{K_0(\zeta_{0n})}e^{in\omega t}\right]\right\}\right), \tag{27}$$

$$\bar{\Xi}_{1,\delta} = \max_t \bar{\Xi}(a+h,t)|_{\delta}, \tag{28}$$

and finally

$$\delta = 1 - \frac{\bar{\Xi}_{1,\delta}}{\bar{\Xi}_{1,0}} \tag{29}$$

is the generalized definition of tethering when the displacement imposed at the inner boundary condition is in the form of a composite wave, as in Eq. (21). The notation $\max_t$ here represents the maximum displacement within one oscillatory cycle of the composite wave. Similar notation for the stress is used in the figures and tables, namely,

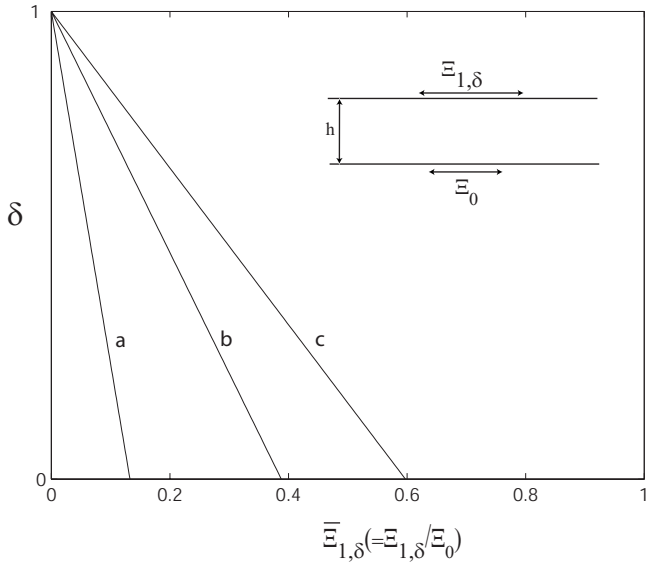

FIG. 4. Displacement amplitude at the outer layer of the vessel wall [Eq. (22)] with different degrees of tethering (δ) and for different categories of wall material: viscous (a), viscoelastic (b), and rigid (c) as defined in Table I. As shown in the inset, $\Xi_{1,\delta}$ is the outer layer displacement amplitude for a tethered wall and Ξ_0 is the inner layer displacement amplitude which derives from the inner boundary condition and which is the same for the three material categories.

$$\bar{T}_{1,0} = \max_t \bar{T}(a+h,t)|_{\delta=0}, \tag{30}$$

$$\bar{T}_{1,\delta} = \max_t \bar{T}(a+h,t)|_{\delta}. \tag{31}$$

For comparison, the corresponding results based on the *approximate* boundary condition in Eq. (8) are given by

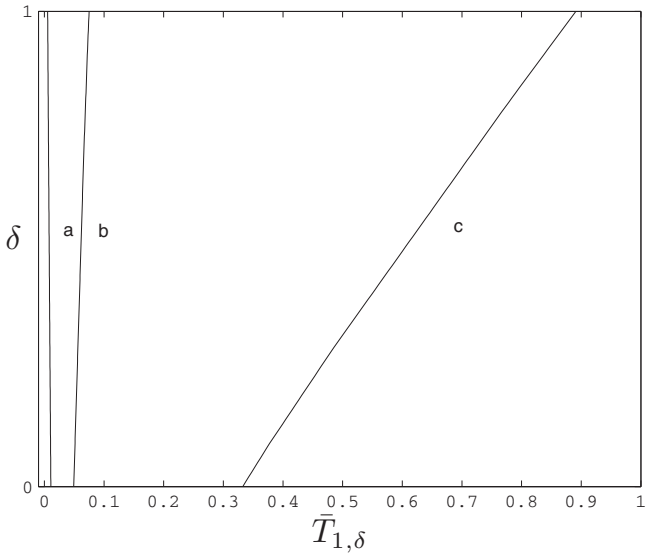

FIG. 5. Shear stress amplitude at the outer layer of the vessel wall [from Eq. (23)] with different degrees of tethering (δ) and for different categories of wall material: viscous (a), viscoelastic (b), and rigid (c) as defined in Table I.

TABLE I. Parameter values used for the three categories of vessel wall materials.

	E_0/E_1	α	β	η_1/E_1	η_2/E_1	$E^*(\omega=1\ \text{Hz})$
Viscous	0	1	1	0.0007	0.0007	$0.004i$
Viscoelastic	0.1	0.11	0.8	0.005	0.005	$0.12+0.014i$
Rigid	1	0	0	0.05	0.05	1.24

$$\bar{\Xi}(r,t) = \frac{1}{\Xi_0}\sum_{n=1}^{10} M_n \Re\{[A_{2n}I_0(\zeta_n) + B_{2n}K_0(\zeta_n)]e^{in\omega t}\} + \frac{1}{\Xi_0}\sum_{n=1}^{10} N_n \Im\{[A_{2n}I_0(\zeta_n) + B_{2n}K_0(\zeta_n)]e^{in\omega t}\} \tag{32}$$

and

$$\bar{T}(r,t) = \frac{1}{\Xi_0}\sum_{n=1}^{10} M_n \Re\{\Lambda_n\lambda_n[A_{2n}I_1(\zeta_n) - B_{2n}K_1(\zeta_n)]e^{in\omega t}\} + \frac{1}{\Xi_0}\sum_{n=1}^{10} N_n \Im\{\Lambda_n\lambda_n[A_{2n}I_1(\zeta_n) - B_{2n}K_1(\zeta_n)]e^{in\omega t}\}, \tag{33}$$

where

$$A_{2n} = \frac{K_1(\zeta_{1n}) - \Lambda_n K_0(\zeta_{1n})}{K_0(\zeta_{0n})[I_1(\zeta_{1n}) + \Lambda_n I_0(\zeta_{1n})] + I_0(\zeta_{0n})[K_1(\zeta_{1n}) - \Lambda_n K_0(\zeta_{1n})]},$$

$$B_{2n} = \frac{I_1(\zeta_{1n}) + \Lambda_n I_0(\zeta_{1n})}{K_0(\zeta_{0n})[I_1(\zeta_{1n}) + \Lambda_n I_0(\zeta_{1n})] + I_0(\zeta_{0n})[K_1(\zeta_{1n}) - \Lambda_n K_0(\zeta_{1n})]}, \tag{34}$$

and

$$\bar{\Xi}(r,t) = \frac{\Xi(r,t)}{\Xi_0}, \tag{35}$$

$$\bar{T}(r,t) = \frac{hT(r,t)}{E_1\Xi_0}. \tag{36}$$

IX. RESULTS AND COMPARISON WITH APPROXIMATE SOLUTION

In general, our results indicate that the oscillatory shear force exerted by blood flow on the endothelial layer of the vessel wall, and the arresting effect of perivascular tissue on the outer layer of the wall together induce longitudinal displacements and stresses within the vessel wall, which depend critically on the viscoelasticity of the wall material and on the degree of tethering. Comparison of our results with those based on the approximate boundary condition is possible only in the case of zero tethering. The difference between the two is significant as seen in Figs. 1 and 2.

The way in which the displacement of the outer layer of an untethered wall of thickness h is obtained from the limiting case of a semi-infinite wall fully tethered at infinity, thus providing the missing outer boundary condition for the former, is illustrated in Fig. 3.

Figures 4 and 5 show the amplitudes of maximum displacement and shear stress, respectively, at the outer layer of the vessel wall for different materials and different degrees of tethering. With zero tethering ($\delta=0$), the outer layer undergoes maximum displacement and minimum shear stress. With full tethering ($\delta=1$), the displacement is zero at the outer layer and the shear stress is maximum. With the same degree of tethering but different wall materials, the displacement and stress is greater with higher elasticity and smaller with higher viscosity.

Table I provides the parameter values of the three wall materials on which the results are based: (i) purely viscous (zero elasticity), (ii) viscoelastic, and (iii) rigid (zero viscosity). The last column shows a reference value of the dynamic

TABLE II. Normalized displacement amplitudes $\bar{\Xi}_{1,\delta}$ at the outer layer of the vessel wall, for different degrees of tethering δ and different material categories.

$\bar{\Xi}_{1,\delta}$	$\delta=0$	$\delta=0.25$	$\delta=0.5$	$\delta=0.75$	$\delta=1$
Viscous	0.13	0.10	0.07	0.03	0
Viscoelastic	0.39	0.29	0.20	0.10	0
Rigid	0.60	0.45	0.30	0.15	0

TABLE III. Normalized shear stress amplitudes $\bar{T}_{1,\delta}$ at the outer layer of the vessel wall, for different degrees of tethering δ and different material categories.

$\bar{T}_{1,\delta}$	$\delta=0$	$\delta=0.25$	$\delta=0.5$	$\delta=0.75$	$\delta=1$
Viscous	0.012	0.009	0.008	0.007	0.006
Viscoelastic	0.05	0.06	0.06	0.07	0.08
Rigid	0.33	0.46	0.60	0.74	0.89

modulus E^* at a frequency of 1 Hz, but it is important to note that in general and for living tissue E^* is actually a function of frequency [15].

In Table II we present the amplitude of the outer layer maximum displacement in different wall materials and for different degrees of tethering, and the corresponding values of the shear stress are given in Table III. In general, as tethering increases, displacements decrease and stresses increase. The only exception is in the case of a purely viscous material because of the missing elastic content and the small value of the dynamic modulus ($E^*=0.004i$ for $\omega=1$ Hz).

X. CONCLUSIONS

The missing outer boundary condition of an untethered arterial wall of finite thickness in pulsatile blood flow can be obtained by considering the limiting case of a semi-infinite wall fully tethered at infinity. The results, using the full equation of motion, provide more accurate values of longitudinal displacements and stresses within the vessel wall than has been possible in the past based on an approximate boundary condition.

The degree of tethering imposed by surrounding tissue can be defined more accurately in terms of the displacement of the outer layer of the vessel wall which with new technology can actually be measured [10], rather than in terms of equivalent added mass which cannot be quantified. Displacement of the outer layer of a partially tethered wall, relative to that in which the wall is untethered and which our results have now determined, provide a more accurate definition of the degree of tethering of the partially tethered wall.

This approach makes it possible for the first time to describe the effects of partial tethering in its full range, from zero to full tethering. The results indicate that high tethering leads to high stresses and low displacements within the vessel wall, while low tethering leads to low stresses and high displacements. Since both extremes would be damaging to wall tissue, particularly elastin, this suggests that moderate tethering would be optimum in the physiological setting. This is consistent with the observation that in different parts of the cardiovascular system arteries are generally tethered to various degrees but are rarely totally tethered or totally untethered.

The analytical solutions on which our results are based have been made possible only by the separation of longitudinal and radial effects and the assumption of a homogeneous wall material, both of which impose obvious limitations on this approach. However, the approach has been valuable in achieving the main objectives of our study, namely, the definition of tethering and the missing boundary condition. To extend this approach to a multilayered wall would clearly require some modifications in order to take into account the different displacements occurring at the interfaces between the layers.

[1] J. D. Humphrey and S. Na, Ann. Biomed. Eng. **30**, 509 (2002).
[2] J. R. Womersley, *Oscillatory Flow in Arteries: The Constrained Elastic Tube as a Model of Arterial Flow and Pulse Transmission* (Wright Air Development Center, Dayton, Ohio, 1955).
[3] G. W. Morgan and W. R. Ferrante, J. Acoust. Soc. Am. **27**, 715 (1955).
[4] G. A. Holzapfel, T. C. Gasser, and M. Stadler, Eur. J. Mech. A/Solids **21**, 441 (2002).
[5] M. Cinthio, A. R. Ahlgren, J. Bergkvist, T. Jansson, H. W. Persson, and K. Lindstrom, Am. J. Physiol. **291**, H394 (2006).
[6] S. Cirovic, C. Walsh, and W. D. Fraser, J. Fluids Structures **16**, 1029 (2002).
[7] D. J. Patel and D. Fry, Circ. Res. **19**, 1011 (1966).
[8] H. B. Atabek, Biophys. J. **8**, 626 (1968).
[9] J. C. Misra and K. R. Choudhury, Rheol. Acta **23**, 548 (1984).
[10] J. E. Wagenseil, N. L. Nerurkar, R. H. Knutsen, R. J. Okamoto, D. Y. Li, and R. P. Mecham, Am. J. Physiol. Heart Circ. Physiol. **289**, H1209 (2005).
[11] D. C. Gazis, J. Acoust. Soc. Am. **31**, 568 (1959).
[12] K. Jagielska, D. Trzupek, M. Lepers, A. Pelc, and P. Zielinski, Phys. Rev. E **76**, 066304 (2007).
[13] H. Wang and K. Williams, J. Sound Vib. **191**, 955 (1996).
[14] S. Hodis and M. Zamir, Phys. Rev. E **78**, 021914 (2008).
[15] D. Craiem and R. L. Armentano, Biorheology **44**, 251 (2007).
[16] M. Zamir, *The Physics of Pulsatile Flow* (Springer-Verlag, New York, 2000).
[17] D. T. Blackstock, *Fundamentals of physical acoustics* (Wiley, New York, 2000).